

# 1 **Global and network functional connectivity of Nucleus Basalis** 2 **of Meynert is strengthened in blind individuals**

3 Ji Won Bang<sup>1\*</sup>, Russell W. Chan<sup>1</sup>, Carlos Parra<sup>1</sup>, Joel S. Schuman<sup>1</sup>, Amy C. Nau<sup>5</sup>, Kevin C. Chan<sup>1-4\*</sup>

4

5 <sup>1</sup>Department of Ophthalmology, NYU Grossman School of Medicine, NYU Langone Health, New  
6 York University, New York, New York, USA;

7 <sup>2</sup>Department of Radiology, NYU Grossman School of Medicine, NYU Langone Health, New York  
8 University, New York, New York, USA;

9 <sup>3</sup>Neuroscience Institute, NYU Grossman School of Medicine, NYU Langone Health, New York  
10 University, New York, New York, USA;

11 <sup>4</sup>Center for Neural Science, College of Arts and Science, New York University, New York, New  
12 York, USA.

13 <sup>5</sup>Korb and Associates, Boston, Massachusetts, USA.

14

15 \*Co-Correspondence to:

16

17 Ji Won Bang, Ph.D.  
18 222 E 41st Street, Room 360  
19 Department of Ophthalmology  
20 NYU Grossman School of Medicine  
21 NYU Langone Health  
22 New York University, New York, NY, USA 10017  
23 Tel: (929) 455-5049 Fax: (212) 263-8749  
24 Email: JiWon.Bang@nyulangone.org

25

26 and

27

28 Kevin C. Chan, Ph.D.  
29 222 E 41st Street, Room 362  
30 Departments of Ophthalmology and Radiology  
31 NYU Grossman School of Medicine  
32 NYU Langone Health  
33 New York University, New York, NY, USA 10017  
34 Tel: (212) 263-7602 Fax: (212) 263-8749  
35 Email: chuenwing.chan@fulbrightmail.org

36 **Total number of figures/tables:** 5 figures/1 table

37

38 **Acknowledgments**

39 This work is supported in part by the National Institutes of Health R01-EY028125 (Bethesda,  
40 Maryland), BrightFocus Foundation G2021001F (Clarksburg, Maryland), Research to Prevent  
41 Blindness/Stavros Niarchos Foundation International Research Collaborators Award (New York,  
42 New York), and an unrestricted grant from Research to Prevent Blindness to NYU Langone Health  
43 Department of Ophthalmology (New York, New York).

44

45 **Declaration of Conflicting Interests**

46 The authors declare no conflict of interests.

47

48 **Abstract**

49 Vision loss causes dramatic changes in brain function which are thought to facilitate behavioral  
50 adaptation. One interesting prospect is that the cholinergic signals are involved in this  
51 blindness-induced plasticity. Critically, the nucleus basalis of Meynert is the principal source of  
52 the cholinergic signals, however, no studies have yet investigated whether the nucleus basalis  
53 of Meynert is altered in blindness. Therefore, here we examined its structure, cerebrovascular  
54 response, and the resting-state functional connectivity in blind individuals. We found that the  
55 global signal of the nucleus basalis of Meynert as well as its network connectivity with the  
56 visual, language, and default mode network is significantly enhanced in early blind individuals.  
57 On the other hand, its structure and cerebrovascular response remain unchanged in early blind  
58 individuals. Further, we observed that less visual experience predicts stronger global and  
59 network connectivity of the nucleus basalis of Meynert. These results suggest that the nucleus  
60 basalis of Meynert develops a stronger neuromodulatory influence on the cortex of blind  
61 individuals at both global and network levels.

62

63

64

65

66

67

68

69

70

71 **Keywords:** nucleus basalis of Meynert, blindness, global connectivity, network connectivity,  
72 resting-state, fMRI, plasticity, choline, plasticity

73

74 **Introduction**

75

76 The brain retains a profound amount of plasticity which enables us to adapt to environmental  
77 demands (Bang and others 2021; Bruel-Jungerman and others 2007). Particularly, loss of vision  
78 has been a critical model for investigating brain plasticity. Ample amount of evidence indicates  
79 that blind individuals perform better than sighted people at various non-visual tasks including  
80 echolocation (Lessard and others 1998; Voss and others 2004), pitch discrimination (Gougoux  
81 and others 2004), speech discrimination (Niemeyer and Starlinger 1981), verbal memory  
82 (Amedi and others 2003; Hull and Mason 1995) and tactile discrimination (Goldreich and Kanics  
83 2003; Van Boven and others 2000).

84

85 One of the influential mechanisms proposed to explain this superior ability of blind individuals is  
86 that compensatory alterations occur in the brain which enhance the processing of non-visual  
87 input (Fine and Park 2018). Indeed, compelling evidence indicates that the blind individuals'  
88 visual cortex becomes recruited for a wide range of non-visual tasks such as Braille reading  
89 (Burton and others 2002; Kupers and others 2007; Sadato and others 1996), auditory localization  
90 (Norman and Thaler 2019; Voss and others 2006), sensory substitution tasks (Murphy and others  
91 2016; Nau and others 2015; Ptito and others 2005; Striem-Amit and others 2012), verbal memory  
92 (Amedi and others 2003), language (Bedny and others 2011; Bedny and others 2015), and  
93 mathematics (Amalric and others 2018; Kanjlia and others 2019). When the visual cortex was  
94 disrupted by transcranial magnetic stimulation during the task, the performance was impaired in  
95 blind individuals (Merabet and others 2009). Beyond the visual cortex, the left superior temporal  
96 sulcus, and the fusiform area were shown to be activated to a greater extent during voice

97 discrimination in congenitally blind individuals (Gougoux and others 2009). This line of studies  
98 suggests that the cortical functional reorganization occurs in blindness that may modulate  
99 various behavioral adaptations.

100

101 In particular, cholinergic signals have been suggested to play a role in blindness-induced  
102 compensatory alterations. The nucleus basalis of Meynert (NBM) provides the major source of  
103 cholinergic signals to the cortex. The cholinergic input from NBM innervates diffusively the  
104 cortex including both primary sensory areas and high-order association areas (Mesulam and  
105 others 1983; Mesulam and others 1984). Critically, the cholinergic signals are involved in  
106 attention (Everitt and Robbins 1997; Sarter and others 2005) and experience-dependent  
107 cortical plasticity (Bakin and Weinberger 1996; Froemke and others 2007; Kilgard and  
108 Merzenich 1998). In addition, the cholinergic neurons in NBM are known to rapidly modulate  
109 sensory processing (Goard and Dan 2009; Pinto and others 2013). For example, when NBM is  
110 stimulated electrically or optogenetically, the cortical coding of visual information in V1 is  
111 enhanced (Goard and Dan 2009; Pinto and others 2013) and the performance on a visual task is  
112 improved in animals (Pinto and others 2013).

113

114 Relatedly, the input from NBM is thought to play a key role in orchestrating spontaneous  
115 activity across the brain (Turchi and others 2018). The resting-state fMRI provides a useful  
116 platform to investigate spontaneous brain activity. This spontaneous brain activity is  
117 distinguishable into two qualitatively different signals. The first one is a network signal that is a  
118 specific correlation between different brain areas. This network signal reflects the functionally

119 connected network architecture (Damoiseaux and others 2006). Further, studies showed that  
120 this network signal is constrained by large-scale anatomical connections (Hagmann and others  
121 2008; Honey and others 2009). On the other hand, global signal refers to broadly shared signal  
122 across the neocortex (Scholvinck and others 2010). This global signal is suggested to reflect  
123 large-scale coordination of brain activity (Cole and others 2010). Building on this, a recent study  
124 demonstrated that NBM regulates global signal fluctuations (Turchi and others 2018).  
125 Specifically, when NBM was inactivated, the global signal components ipsilateral to the  
126 injection site were suppressed whereas the specific correlations that define resting-state  
127 networks were unaffected. This finding suggests that the input of NBM contributes to the  
128 global signals but has little influence on the network signals.

129

130 In the field of blindness-induced plasticity, the amount of choline was observed to be higher in  
131 the visual cortex of early blind individuals (Coullon and others 2015; Weaver and others 2013).  
132 An interesting question arises from this observation, namely, whether NBM plays a causal role  
133 in enhancing the cholinergic signals in the blind's visual cortex. This idea is supported by the  
134 fact that NBM sends cholinergic projections to the entire cortex including visual areas  
135 (Mesulam and others 1983; Mesulam and others 1984).

136

137 Here, we propose that NBM develops a stronger influence to the neocortex of blind individuals  
138 in order to facilitate non-visual processing. Using anatomical MRI and resting-state functional  
139 MRI, we provide novel support for this prediction, presenting enhanced global and network  
140 connectivity of NBM during rest in early blind individuals. Particularly, the cortical networks

141 that present increased network connectivity with NBM include visual networks bilaterally  
142 (occipital visual cortex, lateral visual cortex, medial visual cortex), language networks of the left  
143 hemisphere (inferior frontal gyrus (IFG), posterior superior temporal gyrus (pSTG)), and default  
144 mode network (posterior cingulate cortex (PCC)). We further confirmed that these changes in  
145 the network and global connectivity of NBM in early blind individuals are not affected by the  
146 structural or cerebrovascular changes of NBM. While these alterations of the network  
147 connectivity, as well as global connectivity, are significant only within the early blind individuals,  
148 the years of visual experience predict both network and global connectivity among early blind,  
149 late blind individuals, and sighted controls. These results suggest that NBM may develop  
150 stronger cholinergic innervations onto the cortex to support behavioral adaptation in blind  
151 individuals.

152

153

154 **Materials and Methods**

155 Participants

156 Forty-nine subjects (23 females, mean age  $54.67 \pm 2.12$ ) without any history of neurological  
157 disorders participated in the study. Seven subjects were congenitally blind, sixteen subjects  
158 were late-blind individuals, and twenty-six subjects were sighted controls. One among late blind  
159 individuals was later excluded from the entire analysis because the functional MR scan failed to  
160 cover NBM. Additional one early blind individual was excluded from the rCVR analysis due to a  
161 problem in rCVR computation but included for other analyses. The demographic data of the  
162 early and late blind individuals are depicted in Table 1. This study was approved by the  
163 Institutional Review Board of Pittsburgh University. All subjects provided written informed  
164 consent.

165



Gender	Age (years)	Onset age (years)	Duration of blindness (years)	Cause
M	58	51	7	Traumatic accident
F	59	53	6	Congenital cataracts, aniridia, pediatric glaucoma
F	53	28	25	diabetic retinopathy
M	62	51	11	Traumatic accident
F	64	0	64	congenital
M	25	0	25	congenital
F	58	0	58	congenital
F	35	31	4	Traumatic accident
M	55	35	20	Trauma accident
M	56	0	56	congenital
M	58	7	51	encephalitis
F	58	46	12	glaucoma
M	18	13	5	pigmentosa
F	60	0	60	retinopathy of prematurity
F	62	0	62	congenital
F	71	59	12	glaucoma
F	60	31	29	glaucoma
M	75	59	16	pigmentosa
F	39	17	22	retinopathy of prematurity
F	30	23	7	tumors
M	63	0	63	retinopathy of prematurity
M	64	54	10	detached retinas

166

167 **Table 1.** Subject demographic and clinical information

168

169 MRI data acquisition

170 MRI data were collected with a 3 T Siemens Allegra MR scanner. Anatomical MR images were

171 obtained using a T1-weighted MPRAGE (176 contiguous 1-mm sagittal slices, voxel size = 1×1×1

172 mm<sup>3</sup>, repetition time (TR) = 1400 ms, echo time (TE) = 2.5 ms, field of view (FOV) = 256×256

173 mm<sup>2</sup>, flip angle = 8°, acquisition matrix = 256×256). Functional images were obtained using a

174 single-shot gradient-echo echo-planar imaging (EPI) sequence (36 contiguous 3-mm axial slices,

175 voxel size =  $2 \times 2 \times 3 \text{ mm}^3$ , TR = 2000 ms, TE = 25 ms, FOV =  $205 \times 205 \text{ mm}^2$ , acquisition matrix =  
176  $64 \times 64$ ) while subjects were at rest with eyes closed. The slices covered the whole brain.

177

#### 178 MRI Voxel-based morphometry (VBM) analysis

179 We conducted VBM analysis to test whether NBM presents any atrophy within the grey and  
180 white matter. T1-weighted MRI images were segmented and normalized to MNI space using  
181 SPM12 (<http://www.fil.ion.ucl.ac.uk/spm/>). Then, the images were smoothed using a Gaussian  
182 kernel of 6mm FWHM.

183

#### 184 Resting-state fMRI analysis

185 T1-weighted MRI and resting-state fMRI images were preprocessed using CONN's default MNI  
186 pipeline in CONN toolbox, version 18.a ([www.nitrc.org/projects/conn,RRID:SCR\\_009550](http://www.nitrc.org/projects/conn,RRID:SCR_009550))  
187 (Whitfield-Gabrieli and Nieto-Castanon 2012). The default preprocessing steps included the  
188 functional realignment and unwarping, slice-timing correction, functional outlier detection,  
189 functional segmentation and normalization, structural segmentation and normalization,  
190 functional smoothing using a Gaussian kernel of 8mm FWHM. The noise components from  
191 cerebral white matter, cerebrospinal fluid, estimated subject-motion parameters, scrubbing,  
192 and linear session effects were removed from the functional images for each voxel and each  
193 subject using an anatomical component-based noise correction procedure (aCompCor)  
194 implemented in CONN's default de-noising pipeline. The functional images were then band-  
195 pass filtered to 0.008 Hz – 0.09 Hz.

196

197 The map of NBM on MNI space was obtained from SPM Anatomy toolbox version 3.0  
198 (Zaborszky and others 2008). In particular, this NBM map was created based on stereotaxic  
199 probabilistic maps of the basal forebrain. Magnocellular cell groups in the subcommissural-  
200 sublenticular region of the basal forebrain were delineated and then warped to the MNI space  
201 (Zaborszky and others 2008). The functional connectivity of the seed NBM was then computed  
202 using CONN toolbox. For global correlation analysis, we calculated the average of correlation  
203 coefficients between each voxel and the rest voxels of the brain across time series. Then we  
204 extracted the global correlation coefficients from the voxels corresponding to seed NBM and  
205 averaged them across the seed voxels to identify NBM's brain-wide correlation properties. For  
206 ROI-level analysis, we used 30 cortical networks that CONN generated. These include default  
207 mode network (bilateral lateral parietal cortex, medial prefrontal cortex, posterior cingulate  
208 cortex), dorsal attention network (bilateral frontal eye fields, bilateral intraparietal sulcus),  
209 frontoparietal network (bilateral lateral prefrontal cortex, bilateral posterior parietal cortex),  
210 language network (bilateral inferior frontal gyrus, bilateral posterior superior temporal gyrus),  
211 salience network (anterior cingulate cortex, bilateral anterior insular cortex, bilateral rostral  
212 prefrontal cortex, bilateral supramarginal gyrus), sensorimotor network (bilateral lateral  
213 sensorimotor cortex, superior sensorimotor cortex), and visual network (bilateral lateral visual  
214 cortex, medial visual cortex, occipital visual cortex). We computed the correlation coefficients  
215 between the seed NBM and all 30 cortical networks and converted them to z-value using  
216 Fisher's r-to-z transformation (Lowe and others 1998). For voxel-level analysis, the correlation  
217 coefficients were obtained between the seed NBM and each voxel and were converted to z-  
218 value using Fisher's r-to-z transformation.

219

220 rCVR analysis

221 rCVR maps were obtained from the resting-state fMRI images using MriCloud

222 (<https://mricloud.org/>). Following prior methods (Liu and others 2017), we computed the voxel-

223 wise CVR index ( $\alpha$ ) using a general linear model between normalized BOLD time series

224 ( $\Delta$ BOLD/BOLD) and the global signal time series ( $GS$ ). Then we calculated the voxel-wise rCVR

225 by normalizing  $\alpha$  by tissue signal intensity averaged across the whole brain ( $SI$ ). The residuals

226 term ( $\beta$ ) was not used for analysis. Below is the summary of these steps.

227 
$$\text{rCVR} = \frac{\alpha}{SI} \text{ where } \alpha \text{ is obtained from } \frac{\Delta\text{BOLD}}{\text{BOLD}} = \alpha \cdot GS + \beta$$

228

229 We extracted rCVR values from NBM and 30 cortical networks which are in MNI space.

230

231 Statistics

232 For all statistical analyses, we used two-tailed parametric tests with statistical significance set at

233  $P < 0.05$ . We assessed the assumption of sphericity for all measures ANCOVAs using Mauchly's

234 sphericity tests. When the assumption of sphericity was violated, we reported Huynh-Feldt

235 corrected results. In the following post-hoc tests, we used Bonferroni method to correct the

236 multiple comparisons and reported Bonferroni-corrected P values. For whole-brain voxel-level

237 analysis, a voxel height threshold of  $p < 0.001$  and a cluster height threshold of  $p\text{-FDR}$

238 corrected  $< 0.05$  were used.

239

240

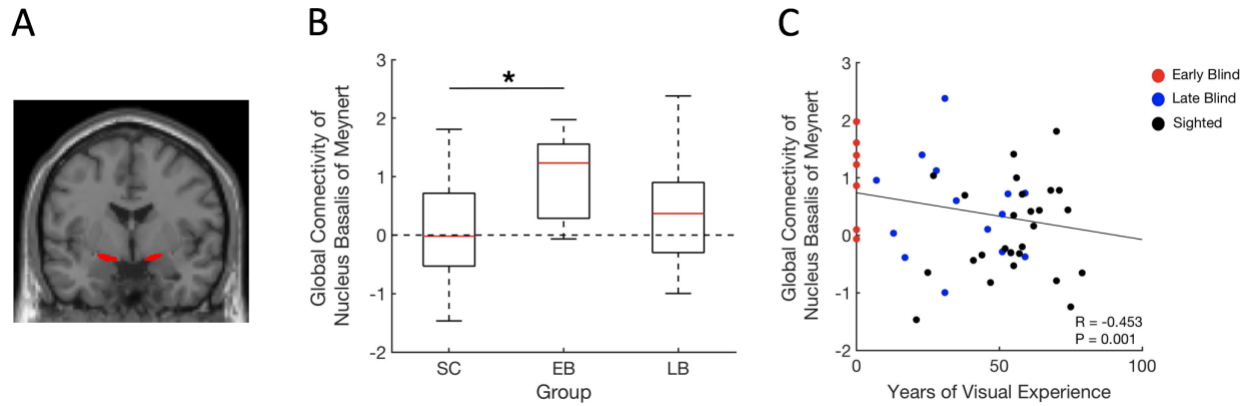
## 241 Results

242 We first examined whether the white and grey matter of NBM (**Fig. 1A**) are altered in blindness  
243 using VBM analysis. For this, we applied a one-way ANCOVA with a factor group (control, early  
244 blind, late blind) to the white and grey matter volumes of NBM as controlling for total  
245 intracranial volume and age. The results revealed no significant main effect of group for both  
246 white and grey matter (white matter volume:  $F(2,43)=1.705$ ,  $P=0.194$ , partial  $\eta^2=0.073$ ; grey  
247 matter volume:  $F(2,43)=1.063$ ,  $P=0.354$ , partial  $\eta^2=0.047$ ), suggesting that the anatomical  
248 structure of NBM remains intact in blindness.

249

250 Next, we investigated whether NBM presents enhanced global signals in blind individuals. To  
251 test for this effect, we computed the global connectivity between NBM and all other cortical  
252 voxels. Then, we conducted a one-way ANCOVA with a factor group (control, early blind, late  
253 blind) controlling for age. The results showed a significant main effect of group ( $F(2,45)=3.530$ ,  
254  $P=0.038$ , partial  $\eta^2=0.136$ ; **Fig. 1B**). Further post-hoc tests showed that the early blind group has  
255 significantly greater global connectivity compared to sighted controls (control vs. early blind,  
256  $P=0.034$ , 95% CI=-1.814 – -0.055). However, this increased global connectivity of NBM in the  
257 early blind group did not differ from that in the late blind group (early blind vs. late blind,  
258  $P=0.248$ , 95% CI=-0.268 – 1.605; control vs. late blind,  $P=0.957$ , 95% CI=-0.923 – 0.391). Further,  
259 we examined whether the global connectivity of NBM is associated with the years of visual  
260 experience by conducting a partial correlation analysis controlling for age. The results showed  
261 that less visual experience predicts a stronger global signal of NBM ( $r=-0.453$ ,  $p=0.001$ ; **Fig. 1C**).

262



263  
264 **Fig. 1.** The Nucleus Basalis of Meynert. (A) Coronal view of the nucleus basalis of Meynert. (B)  
265 Global connectivity between the nucleus basalis of Meynert and the entire cortical areas is  
266 significantly increased in the early blind group compared to sighted controls. The distributions  
267 are represented using box plots. “SC”, “EB,” and “LB” refer to the sighted controls, early blind  
268 and late blind groups. \* Bonferroni-corrected  $P < 0.05$ . (C) Years of visual experience predict  
269 global connectivity of nucleus basalis of Meynert. Each point represents one subject. Red, blue  
270 and black colors indicate early blind, late blind, and sighted controls. The R and P values in the  
271 figure refer to the result of a partial correlation test between years of visual experience and  
272 global connectivity of nucleus basalis of Meynert controlling for age.  $N=48$ .  
273

274 Having confirmed the enhanced global signal of NBM in early blind individuals, we further  
275 examined whether early blind individuals have increased network connectivity as well. We  
276 addressed this question using ROI- and voxel-based analyses. For ROI-based analysis, we  
277 created 30 cortical network ROIs (see Materials and Methods) and computed the functional  
278 connectivity between NBM and each of the network ROIs. We then conducted a two-way mixed  
279 measures ANCOVA with factors group (control, early blind, late blind) and network (30 cortical  
280 networks) to the functional connectivity controlling for age. The results revealed a significant  
281 main effect of group ( $F(2,44)=9.339$ ,  $P<0.001$ , partial  $\eta^2=0.298$ ) and significant interaction  
282 between group and network ( $F(58,1276)=1.754$ , Huynh-Feldt correction,  $P=0.015$ , partial  
283  $\eta^2=0.074$ ) but no main effect of network ( $F(29,1276)=0.952$ ,  $P=0.494$ , partial  $\eta^2=0.021$ ).  
284 Following post-hoc tests showed that the functional connectivity of the early blind individuals is

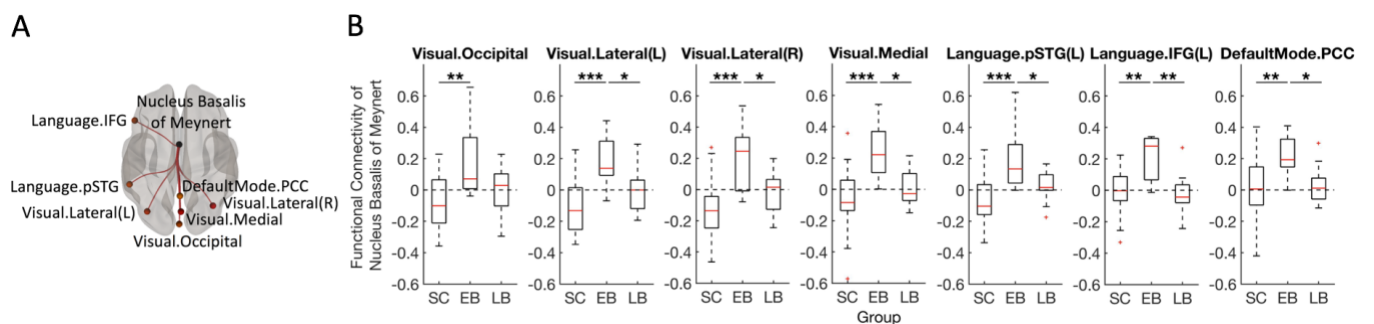
285 greater than that of the sighted controls and late blind individuals (control vs. early blind:  
286  $P < 0.001$ , 95% CI = -0.160 – -0.043; control vs. late blind:  $P = 0.760$ , 95% CI = -0.065 – 0.024; early  
287 blind vs. late blind:  $P = 0.008$ , 95% CI = 0.018 – 0.143). Further, a significant interaction between  
288 group and network suggests that the functional connectivity changes across the group and that  
289 this pattern of change differs across networks.

290

291 Given the significant interaction between group and network, we examined more in detail how  
292 the functional connectivity changes across networks by conducting a one-way ANCOVA with a  
293 factor group (control, early blind, late blind) to each network as controlling for age. The results  
294 revealed a significant main effect of group at visual networks bilaterally (occipital visual cortex:  
295  $F(2, 44) = 5.491$ ,  $P = 0.007$ , partial  $\eta^2 = 0.200$ ; left lateral visual cortex:  $F(2, 44) = 8.853$ ,  $P = 0.001$ ,  
296 partial  $\eta^2 = 0.287$ ; right lateral visual cortex:  $F(2, 44) = 10.818$ ,  $P < 0.001$ , partial  $\eta^2 = 0.330$ ; medial  
297 visual cortex:  $F(2, 44) = 9.861$ ,  $P < 0.001$ , partial  $\eta^2 = 0.310$ ; **Fig. 2B**), language networks of the left  
298 hemisphere (left posterior superior temporal gyrus:  $F(2, 44) = 10.413$ ,  $P < 0.001$ , partial  $\eta^2 = 0.321$ ;  
299 left inferior frontal gyrus:  $F(2, 44) = 8.105$ ,  $P = 0.001$ , partial  $\eta^2 = 0.269$ ; **Fig. 2B**), and default mode  
300 network (posterior cingulate cortex:  $F(2, 44) = 5.245$ ,  $P = 0.009$ , partial  $\eta^2 = 0.193$ ; **Fig. 2B**).

301 Following post-hoc tests showed that in the occipital visual cortex, the early blind group has  
302 higher functional connectivity compared to sighted controls (control vs. early blind:  $P = 0.006$ ,  
303 95% CI = -0.441 – -0.060; control vs. late blind:  $P = 0.542$ , 95% CI = -0.224 – 0.066; early blind vs.  
304 late blind:  $P = 0.129$ , 95% CI = -0.033 – 0.376). In the left lateral visual cortex, the functional  
305 connectivity of the early blind group is higher than that of the sighted controls and late blind  
306 group (control vs. early blind:  $P < 0.001$ , 95% CI = -0.465 – -0.117; control vs. late blind:  $P = 0.236$ ,

307 95% CI=-0.229 – 0.037; early blind vs. late blind: P=0.040, 95% CI=0.007 – 0.383). Similar post-  
 308 hoc results, that is significantly increased functional connectivity of the early blind group  
 309 compared to that of the sighted controls and late blind group were observed in the right lateral  
 310 visual cortex (control vs. early blind: P<0.001, 95% CI=-0.533 – -0.155; control vs. late blind:  
 311 P=0.083, 95% CI=-0.276 – 0.012; early blind vs. late blind: P=0.039, 95% CI=0.008 – 0.416),  
 312 medial visual cortex (control vs. early blind: P<0.001, 95% CI=-0.492 – -0.138; control vs. late  
 313 blind: P=0.389, 95% CI=-0.219 – 0.051; early blind vs. late blind: P=0.013, 95% CI=0.041 –  
 314 0.422), left posterior superior temporal gyrus (control vs. early blind: P<0.001, 95% CI=-0.421 – -  
 315 0.119; control vs. late blind: P=0.098, 95% CI=-0.218 – 0.013; early blind vs. late blind: P=0.041,  
 316 95% CI=0.005 – 0.331), left inferior frontal gyrus (control vs. early blind: P=0.002, 95% CI=-0.373  
 317 – -0.75; control vs. late blind: P=1.000, 95% CI=-0.097 – 0.131; early blind vs. late blind:  
 318 P=0.002, 95% CI=0.081 – 0.402), and posterior cingulate cortex (control vs. early blind: P=0.008,  
 319 95% CI=-0.359 – -0.044; control vs. late blind: P=1.000, 95% CI=-0.134 – 0.107; early blind vs.  
 320 late blind: P=0.026, 95% CI=0.018 – 0.357).



321  
 322

323 **Fig. 2.** Early blind individuals have increased functional connectivity between nucleus basalis of  
 324 Meynert and cortical networks including visual networks, language networks, and default mode  
 325 network. (A) Schematic depiction of the nucleus basalis of Meynert and seven cortical networks  
 326 (occipital, lateral, medial visual cortices, left posterior superior temporal gyrus, left inferior  
 327 frontal gyrus, posterior cingulate cortex) which showed enhanced connectivity with the nucleus  
 328 basalis of Meynert in the early blind group. (B) Functional connectivity between the nucleus  
 329 basalis of Meynert and seven cortical networks. The distributions are represented using box



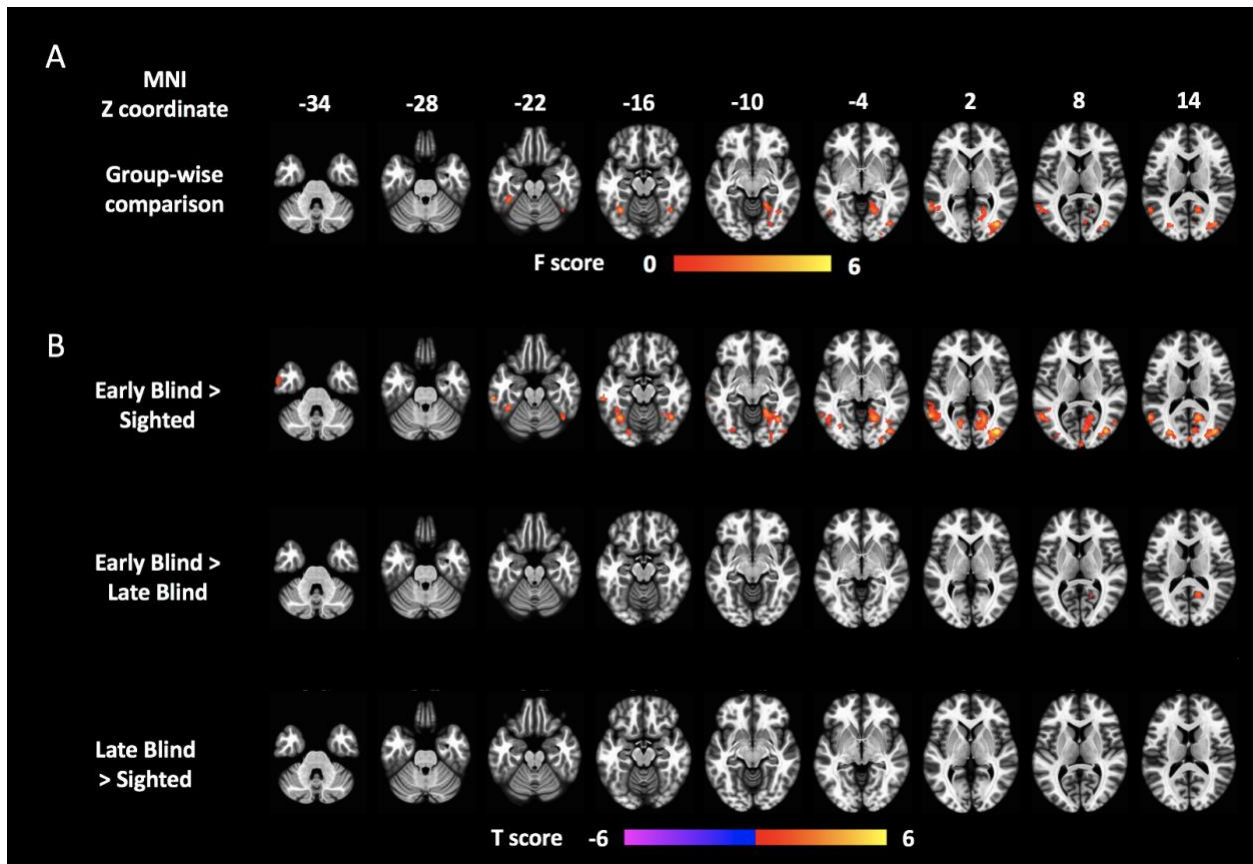
330 plots and the outliers are plotted as plus signs. “SC”, “EB,” and “LB” refer to the sighted  
331 controls, early blind and late blind groups. \* Bonferroni-corrected  $P < 0.05$ , \*\* Bonferroni-  
332 corrected  $P < 0.01$ .  $N=48$ .

333

334

335 The above analyses were conducted on averaged functional connectivity across large-scale  
336 brain networks. For completeness, we also examined the functional network connectivity of  
337 NBM at the voxel level. For this, we computed the functional connectivity between NBM and  
338 each cortical voxel. We then conducted a one-way ANCOVA with a factor group (control, early  
339 blind, late blind) controlling for age. As in the above ROI-level analysis, we observed a  
340 significant main effect of group within the visual cortex bilaterally, and the left middle temporal  
341 gyrus (**Fig. 3A**). Additionally, the voxel-level analysis found group difference in the bilateral  
342 fusiform area, which was previously included in the medial visual network during the ROI-level  
343 analysis. Further post-hoc tests (**Fig. 3B**) revealed that this group difference was driven by the  
344 early blind group. A comparison between early blind and sighted controls revealed that early  
345 blind individuals have greater functional connectivity of NBM at the visual cortex bilaterally,  
346 and left superior, middle, inferior temporal gyrus, as well as fusiform area bilaterally. Another  
347 comparison between early and late blind groups showed that the early blind group has  
348 significantly higher connectivity of NBM at the right visual cortex. On the other hand, late blind  
349 and sighted controls did not yield a significant difference at any voxels. These results replicate  
350 the ROI-level analysis results although the voxel-level analysis did not observe significant  
351 changes within the left inferior frontal gyrus (language network) and the posterior cingulate  
352 cortex (default mode network), possibly due to multiple comparisons correction at the voxel  
353 level.

354



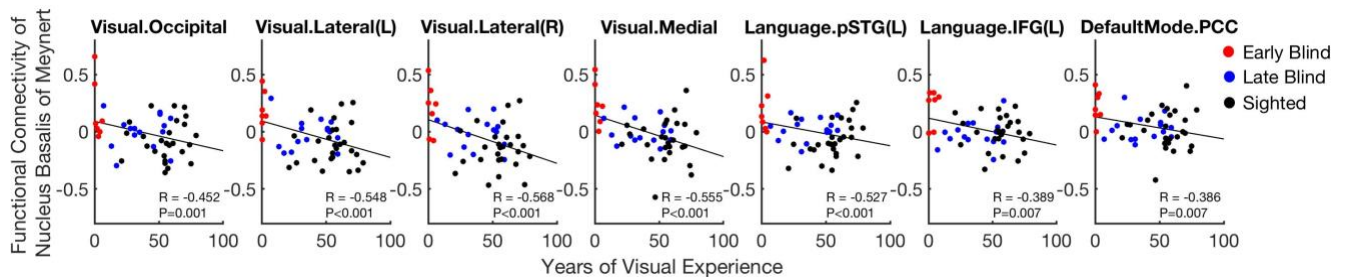
355

356 **Fig. 3.** Group difference of functional connectivity of the nucleus basalis of Meynert. (A) F map  
357 for the group-wise difference. Significant group differences are observed in the bilateral visual  
358 cortex, left middle temporal gyrus, and bilateral fusiform area. (B) Post-hoc group-wise t-tests  
359 between groups. The early blind individuals have increased connectivity of nucleus basalis of  
360 Meynert within the bilateral visual cortex, left superior, middle, inferior temporal gyrus, and the  
361 bilateral fusiform area compared to sighted controls. Another comparison between early and  
362 late blind individuals shows that the early blind group has higher connectivity in the right visual  
363 cortex. The late blind and sighted individuals did not show any significant difference. N=48  
364

365

366 Since the voxel-level results replicate the findings of the ROI-level analysis, we further explored  
367 whether the increase of functional connectivity between NBM and cortical networks is  
368 negatively associated with the years of visual experience. For this, we conducted partial  
369 correlation analyses controlling for age, using six cortical networks which showed enhanced  
370 connectivity with NBM in the early blind group. The results revealed significant correlations

371 within visual networks (occipital visual network:  $r=-0.452$ ,  $p=0.001$ ; left lateral visual network:  
372  $r=-0.548$ ,  $p<0.001$ ; right lateral visual network:  $r=-0.568$ ,  $p<0.001$ ; medial visual network:  $r=-$   
373  $0.555$ ,  $p<0.001$ ), language networks (left posterior superior temporal gyrus:  $r=-0.527$ ,  $p<0.001$ ;  
374 left inferior frontal gyrus:  $r=-0.389$ ,  $p=0.007$ ), and default mode network (posterior cingulate  
375 cortex:  $r=-0.386$ ,  $p=0.007$ ; **Fig. 4**). The results indicate that less visual experience predicts  
376 greater functional connectivity of NBM within these networks.  
377



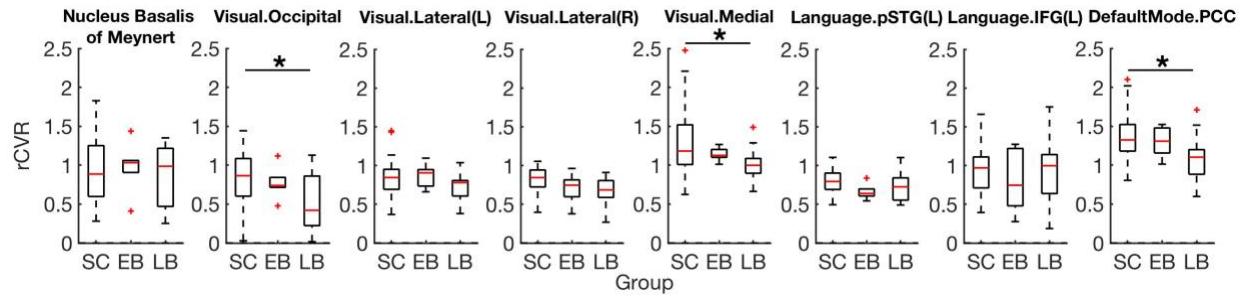
379 **Fig. 4.** Years of visual experience predict functional connectivity of nucleus basalis of Meynert.  
380 Significant correlations were observed within visual networks (occipital, lateral, medial visual  
381 areas), language networks (left posterior superior temporal gyrus, left inferior frontal gyrus),  
382 and default mode network (posterior cingulate cortex). Each point represents one subject. Red,  
383 blue and black colors indicate early blind, late blind, and sighted controls. For visualization  
384 purposes, early-blind data points are plotted apart from each other although their x values are  
385 all 0. The R and P values in the figure refer to the results of partial correlation tests between  
386 years of visual experience and functional connectivity of nucleus basalis of Meynert controlling  
387 for age. N=48.  
388

389  
390 Finally, we examined whether these global and network signals are affected by cerebrovascular  
391 changes using the relative cerebrovascular reactivity (rCVR) map computed from resting-state  
392 fMRI (see Materials and Methods). The rCVR measures the cerebral blood vessels' ability to  
393 dilate or constrict in response to vasoactive stimuli (Liu and others 2019). Since the BOLD  
394 signals in the resting-state fMRI are tightly related to the degree to which cerebral blood

395 vessels respond to the neurovascular coupling chemical signals (Gauthier and Fan 2019), it is  
396 important to examine whether the observed resting-state functional connectivity changes in  
397 the early blind group are influenced by cerebrovascular changes. To test whether there are any  
398 alterations of rCVR within NBM and the cortical networks that showed significant changes in  
399 the early blind group, we applied a one-way ANCOVA with a factor group (control, early blind,  
400 late blind) to the rCVR measures controlling for age. We observed no significant main effect of  
401 group in NBM ( $F(2, 43)=0.257$ ,  $P=0.775$ , partial  $\eta^2=0.012$ ), left lateral visual cortex ( $F(2,$   
402  $43)=2.094$ ,  $P=0.136$ , partial  $\eta^2=0.089$ ), and left inferior frontal gyrus ( $F(2, 43)=0.417$ ,  $P=0.662$ ,  
403 partial  $\eta^2=0.019$ ; **Fig. 5**). However, significant main effect of group was observed in the occipital  
404 visual cortex ( $F(2, 43)=4.114$ ,  $P=0.023$ , partial  $\eta^2=0.161$ ), right lateral visual cortex ( $F(2,$   
405  $43)=3.235$ ,  $P=0.049$ , partial  $\eta^2=0.131$ ), medial visual cortex ( $F(2, 43)=3.292$ ,  $P=0.047$ , partial  
406  $\eta^2=0.133$ ), left posterior superior temporal gyrus ( $F(2, 43)=3.279$ ,  $P=0.047$ , partial  $\eta^2=0.132$ )  
407 and posterior cingulate cortex ( $F(2, 43)=3.725$ ,  $P=0.032$ , partial  $\eta^2=0.148$ ; **Fig. 5**). Further post-  
408 hoc tests revealed that this significant main effect of group is driven by the reduced rCVR of the  
409 late blind individuals, but not by that of the early blind individuals. Specifically, significant  
410 differences between sighted controls and late blind group were observed within the occipital  
411 visual cortex ( $P=0.020$ , 95% CI=0.038 – 0.574), medial visual cortex ( $P=0.045$ , 95% CI=0.005 –  
412 0.576) and the posterior cingulate cortex ( $P=0.029$ , 95% CI=0.023 – 0.535; **Fig. 5**) but not within  
413 the right lateral visual cortex ( $P=0.052$ , 95% CI=-0.001 – 0.297) and left posterior superior  
414 temporal gyrus ( $P=0.220$ , 95% CI=-0.031 – 0.207). The results suggest that the late blind  
415 individuals have impaired rCVR within the occipital, medial visual cortex, and the posterior  
416 cingulate cortex. Critically, comparable rCVRs between early blind individuals and sighted

417 controls suggest that the altered global signal and network connectivity of NBM in early blind  
418 individuals are not due to cerebrovascular changes, but rather that these changes are primarily  
419 driven by the altered neural activity of NBM.

420



421

422 **Fig. 5.** rCVR of the nucleus basalis of Meynert and seven cortical networks that showed  
423 significant change in the early blind group. rCVRs of early blind individuals are comparable to  
424 those of sighted controls whereas rCVR of late blind individuals are significantly lower than  
425 those of sighted controls within the occipital visual cortex, medial visual cortex, and posterior  
426 cingulate cortex. The distributions are represented using box plots and the outliers are plotted  
427 as plus signs. "SC", "EB," and "LB" refer to the sighted controls, early blind and late blind  
428 groups. \* Bonferroni-corrected  $P < 0.05$ .  $N=47$ .

429

430

431 **Discussion**

432 The present results provide robust evidence that spontaneous brain activity of NBM is altered  
433 in early blind individuals while its anatomical structure and cerebrovascular response are  
434 unchanged. Specifically, we observed that both global and network connectivity of NBM is  
435 significantly enhanced in early blind individuals. The cortical networks that present increased  
436 connectivity with NBM include bilateral visual networks, language networks of the left  
437 hemisphere, and the default mode network. Further, the years of visual experience are  
438 significantly correlated with both global and network connectivity among early blind, late blind,  
439 and sighted individuals. These results provide direct evidence that NBM develops greater  
440 neuromodulatory effects on the neocortex of blind individuals, with its strongest effect on early  
441 blind individuals.

442  
443 The cholinergic innervations originating from NBM are known to play a key role in attention  
444 (Everitt and Robbins 1997; Sarter and others 2005), experience-dependent plasticity (Bakin and  
445 Weinberger 1996; Froemke and others 2007; Kilgard and Merzenich 1998), and sensory  
446 processing (Goard and Dan 2009; Pinto and others 2013). At the scale of seconds, the  
447 cholinergic neurons of NBM rapidly modulate the visual processing in V1 (Pinto and others  
448 2013) and the release of choline in the cortex is correlated with behavioral performance (Parikh  
449 and others 2007). Thus, our results of enhanced global and network connectivity of NBM  
450 suggest that blind individuals are under the greater cholinergic influence which underlies the  
451 neural processes of attention, plasticity, and sensory processing. This is consistent with the  
452 prior observation that the blind individuals have superior capacity at various non-visual tasks

453 (Amedi and others 2003; Goldreich and Kanics 2003; Gougoux and others 2004; Lessard and  
454 others 1998; Niemeyer and Starlinger 1981) and that their visual cortex is recruited for non-  
455 visual information processing (Amalric and others 2018; Amedi and others 2003; Murphy and  
456 others 2016; Norman and Thaler 2019; Sadato and others 1996). Indeed, prior studies  
457 demonstrated that the visual cortex of early blind individuals contains a greater amount of  
458 choline (Coullon and others 2015; Weaver and others 2013).

459

460 An important question that arises from our study concerns the role of stronger global  
461 connectivity of NBM in blind individuals. The brain region that has high connectivity with the  
462 rest of the brain suggests that this area is essential for coordinating large-scale brain activity  
463 patterns (Cole and others 2010). Thus, our results suggest that NBM exerts greater influence on  
464 coordinating the large-scale brain activity in blind individuals. This explanation is in line with a  
465 recent observation that NBM modulates the global signals but has minimal effect on the  
466 network connectivity (Turchi and others 2018).

467

468 Although NBM was reported to play little role in the network connectivity (Turchi and others  
469 2018), we observed that NBM has increased network connectivity in blind individuals at  
470 bilateral visual networks, language networks of the left hemisphere, and the default mode  
471 network. Different from global connectivity, the network connectivity contains information  
472 about functionally connected brain structure (Damoiseaux and others 2006). Thus, our results  
473 indicate that NBM is more functionally coupled with the visual, language, and default mode  
474 networks in blind individuals. This enhanced functional connectivity may serve to facilitate

475 cholinergic modulation during tasks. Indeed, the brain areas that showed increased activity  
476 during the non-visual tasks in blind individuals include the visual cortex (Amalric and others  
477 2018; Amedi and others 2003; Bedny and others 2011; Murphy and others 2016; Norman and  
478 Thaler 2019; Sadato and others 1996), fusiform area and the left superior temporal sulcus  
479 (Gougoux and others 2009). These areas overlap with those that showed increased network  
480 connectivity with NBM in the current study. Thus, stronger activation of these cortical areas in  
481 blind individuals observed during tasks is likely to be associated with greater cholinergic  
482 modulation of NBM.

483

484 The current results raise important questions for future studies. First, it remains unclear  
485 whether cholinergic signals in the cortical areas are directly driven by NBM activity in blind  
486 individuals. This question can be partly addressed by quantifying the amount of choline from  
487 the cortex using magnetic resonance spectroscopy and then examining the correlation between  
488 the amount of choline and the functional connectivity between NBM and the corresponding  
489 cortical areas. Secondly, it has not been explored yet whether the NBM regulates the neural  
490 activity in the cortical networks during non-visual tasks in blind individuals. While our results  
491 imply such direct regulation of NBM, we only examined the brain activity during rest, but not  
492 during the task. If further studies reveal direct modulation of NBM during tasks in blind  
493 individuals, its timescales and impact on the performance are the next important questions for  
494 future inquiry.

495



496 To summarize, our results show that the functional connectivity of NBM becomes strengthened  
497 in the absence of visual input at both global and network levels. This alteration appears to arise  
498 from neural changes of NBM, but not from structural or neurovascular changes. These findings  
499 thus suggest that stronger cholinergic modulation of NBM may serve to facilitate behavioral  
500 adaptation in blind individuals.

501

502

503

504

505

506

507 **References**

508

- 509 Amalric M, Degenhien I, Dehaene S. 2018. On the role of visual experience in mathematical  
510 development: Evidence from blind mathematicians. *Dev Cogn Neurosci* 30:314-323.
- 511 Amedi A, Raz N, Pianka P, Malach R, Zohary E. 2003. Early 'visual' cortex activation correlates  
512 with superior verbal memory performance in the blind. *Nat Neurosci* 6(7):758-66.
- 513 Bakin JS, Weinberger NM. 1996. Induction of a physiological memory in the cerebral cortex by  
514 stimulation of the nucleus basalis. *Proc Natl Acad Sci U S A* 93(20):11219-24.
- 515 Bang JW, Hamilton-Fletcher G, Chan KC. 2021. Visual Plasticity in Adulthood: Perspectives from  
516 Hebbian and Homeostatic Plasticity. *Neuroscientist*:10738584211037619.
- 517 Bedny M, Pascual-Leone A, Dodell-Feder D, Fedorenko E, Saxe R. 2011. Language processing in  
518 the occipital cortex of congenitally blind adults. *Proc Natl Acad Sci U S A* 108(11):4429-  
519 34.
- 520 Bedny M, Richardson H, Saxe R. 2015. "Visual" Cortex Responds to Spoken Language in Blind  
521 Children. *J Neurosci* 35(33):11674-81.
- 522 Bruel-Jungerman E, Davis S, Laroche S. 2007. Brain plasticity mechanisms and memory: a party  
523 of four. *Neuroscientist* 13(5):492-505.
- 524 Burton H, Snyder AZ, Conturo TE, Akbudak E, Ollinger JM, Raichle ME. 2002. Adaptive changes  
525 in early and late blind: a fMRI study of Braille reading. *J Neurophysiol* 87(1):589-607.
- 526 Cole MW, Pathak S, Schneider W. 2010. Identifying the brain's most globally connected regions.  
527 *Neuroimage* 49(4):3132-3148.
- 528 Coullon GS, Emir UE, Fine I, Watkins KE, Bridge H. 2015. Neurochemical changes in the  
529 pericalcarine cortex in congenital blindness attributable to bilateral anophthalmia. *J*  
530 *Neurophysiol* 114(3):1725-33.
- 531 Damoiseaux JS, Rombouts SA, Barkhof F, Scheltens P, Stam CJ, Smith SM and others. 2006.  
532 Consistent resting-state networks across healthy subjects. *Proc Natl Acad Sci U S A*  
533 103(37):13848-53.
- 534 Everitt BJ, Robbins TW. 1997. Central cholinergic systems and cognition. *Annu Rev Psychol*  
535 48:649-84.
- 536 Fine I, Park JM. 2018. Blindness and Human Brain Plasticity. *Annu Rev Vis Sci* 4:337-356.
- 537 Froemke RC, Merzenich MM, Schreiner CE. 2007. A synaptic memory trace for cortical receptive  
538 field plasticity. *Nature* 450(7168):425-9.
- 539 Gauthier CJ, Fan AP. 2019. BOLD signal physiology: Models and applications. *Neuroimage*  
540 187:116-127.
- 541 Goard M, Dan Y. 2009. Basal forebrain activation enhances cortical coding of natural scenes.  
542 *Nat Neurosci* 12(11):1444-9.
- 543 Goldreich D, Kanics IM. 2003. Tactile acuity is enhanced in blindness. *Journal of Neuroscience*  
544 23(8):3439-3445.
- 545 Gougoux F, Belin P, Voss P, Lepore F, Lassonde M, Zatorre RJ. 2009. Voice perception in blind  
546 persons: a functional magnetic resonance imaging study. *Neuropsychologia*  
547 47(13):2967-74.
- 548 Gougoux F, Lepore F, Lassonde M, Voss P, Zatorre RJ, Belin P. 2004. Neuropsychology: pitch  
549 discrimination in the early blind. *Nature* 430(6997):309.

- 550 Hagmann P, Cammoun L, Gigandet X, Meuli R, Honey CJ, Wedeen VJ and others. 2008. Mapping  
551 the structural core of human cerebral cortex. *PLoS Biol* 6(7):e159.
- 552 Honey CJ, Sporns O, Cammoun L, Gigandet X, Thiran JP, Meuli R and others. 2009. Predicting  
553 human resting-state functional connectivity from structural connectivity. *Proc Natl Acad*  
554 *Sci U S A* 106(6):2035-40.
- 555 Hull T, Mason H. 1995. Performance of Blind-Children on Digit-Span Tests. *Journal of Visual*  
556 *Impairment & Blindness* 89(2):166-169.
- 557 Kanjlia S, Pant R, Bedny M. 2019. Sensitive Period for Cognitive Repurposing of Human Visual  
558 Cortex. *Cereb Cortex* 29(9):3993-4005.
- 559 Kilgard MP, Merzenich MM. 1998. Cortical map reorganization enabled by nucleus basalis  
560 activity. *Science* 279(5357):1714-8.
- 561 Kupers R, Pappens M, de Noordhout AM, Schoenen J, Ptito M, Fumal A. 2007. rTMS of the  
562 occipital cortex abolishes Braille reading and repetition priming in blind subjects.  
563 *Neurology* 68(9):691-3.
- 564 Lessard N, Pare M, Lepore F, Lassonde W. 1998. Early-blind human subjects localize sound  
565 sources better than sighted subjects. *Nature* 395(6699):278-280.
- 566 Liu P, De Vis JB, Lu H. 2019. Cerebrovascular reactivity (CVR) MRI with CO2 challenge: A  
567 technical review. *Neuroimage* 187:104-115.
- 568 Liu PY, Li Y, Pinho M, Park DC, Welch BG, Lu HZ. 2017. Cerebrovascular reactivity mapping  
569 without gas challenges. *Neuroimage* 146:320-326.
- 570 Lowe MJ, Mock BJ, Sorenson JA. 1998. Functional connectivity in single and multislice  
571 echoplanar imaging using resting-state fluctuations. *Neuroimage* 7(2):119-32.
- 572 Merabet LB, Battelli L, Obretenova S, Maguire S, Meijer P, Pascual-Leone A. 2009. Functional  
573 recruitment of visual cortex for sound encoded object identification in the blind.  
574 *Neuroreport* 20(2):132-8.
- 575 Mesulam MM, Mufson EJ, Levey AI, Wainer BH. 1983. Cholinergic innervation of cortex by the  
576 basal forebrain: cytochemistry and cortical connections of the septal area, diagonal  
577 band nuclei, nucleus basalis (substantia innominata), and hypothalamus in the rhesus  
578 monkey. *J Comp Neurol* 214(2):170-97.
- 579 Mesulam MM, Mufson EJ, Levey AI, Wainer BH. 1984. Atlas of cholinergic neurons in the  
580 forebrain and upper brainstem of the macaque based on monoclonal choline  
581 acetyltransferase immunohistochemistry and acetylcholinesterase histochemistry.  
582 *Neuroscience* 12(3):669-86.
- 583 Murphy MC, Nau AC, Fisher C, Kim SG, Schuman JS, Chan KC. 2016. Top-down influence on the  
584 visual cortex of the blind during sensory substitution. *Neuroimage* 125:932-940.
- 585 Nau AC, Murphy MC, Chan KC. 2015. Use of sensory substitution devices as a model system for  
586 investigating cross-modal neuroplasticity in humans. *Neural Regen Res* 10(11):1717-9.
- 587 Niemeyer W, Starlinger I. 1981. Do the blind hear better? Investigations on auditory processing  
588 in congenital or early acquired blindness. II. Central functions. *Audiology* 20(6):510-5.
- 589 Norman LJ, Thaler L. 2019. Retinotopic-like maps of spatial sound in primary 'visual' cortex of  
590 blind human echolocators. *Proc Biol Sci* 286(1912):20191910.
- 591 Parikh V, Kozak R, Martinez V, Sarter M. 2007. Prefrontal acetylcholine release controls cue  
592 detection on multiple timescales. *Neuron* 56(1):141-54.

593 Pinto L, Goard MJ, Estandian D, Xu M, Kwan AC, Lee SH and others. 2013. Fast modulation of  
594 visual perception by basal forebrain cholinergic neurons. *Nat Neurosci* 16(12):1857-  
595 1863.

596 Ptito M, Moesgaard SM, Gjedde A, Kupers R. 2005. Cross-modal plasticity revealed by  
597 electrotactile stimulation of the tongue in the congenitally blind. *Brain* 128(Pt 3):606-14.

598 Sadato N, Pascual-Leone A, Grafman J, Ibanez V, Deiber MP, Dold G and others. 1996.  
599 Activation of the primary visual cortex by Braille reading in blind subjects. *Nature*  
600 380(6574):526-8.

601 Sarter M, Hasselmo ME, Bruno JP, Givens B. 2005. Unraveling the attentional functions of  
602 cortical cholinergic inputs: interactions between signal-driven and cognitive modulation  
603 of signal detection. *Brain Res Brain Res Rev* 48(1):98-111.

604 Scholvinck ML, Maier A, Ye FQ, Duyn JH, Leopold DA. 2010. Neural basis of global resting-state  
605 fMRI activity. *Proc Natl Acad Sci U S A* 107(22):10238-43.

606 Striem-Amit E, Cohen L, Dehaene S, Amedi A. 2012. Reading with sounds: sensory substitution  
607 selectively activates the visual word form area in the blind. *Neuron* 76(3):640-52.

608 Turchi J, Chang C, Ye FQ, Russ BE, Yu DK, Cortes CR and others. 2018. The Basal Forebrain  
609 Regulates Global Resting-State fMRI Fluctuations. *Neuron* 97(4):940-952 e4.

610 Van Boven RW, Hamilton RH, Kauffman T, Keenan JP, Pascual-Leone A. 2000. Tactile spatial  
611 resolution in blind Braille readers. *Neurology* 54(12):2230-2236.

612 Voss P, Gougoux F, Lassonde M, Zatorre RJ, Lepore F. 2006. A positron emission tomography  
613 study during auditory localization by late-onset blind individuals. *Neuroreport* 17(4):383-  
614 8.

615 Voss P, Lassonde M, Gougoux F, Fortin M, Guillemot JP, Lepore F. 2004. Early- and late-onset  
616 blind individuals show supra-normal auditory abilities in far-space. *Current Biology*  
617 14(19):1734-1738.

618 Weaver KE, Richards TL, Saenz M, Petropoulos H, Fine I. 2013. Neurochemical Changes within  
619 Human Early Blind Occipital Cortex. *Neuroscience* 252:222-233.

620 Whitfield-Gabrieli S, Nieto-Castanon A. 2012. Conn: a functional connectivity toolbox for  
621 correlated and anticorrelated brain networks. *Brain Connect* 2(3):125-41.

622 Zaborszky L, Hoemke L, Mohlberg H, Schleicher A, Amunts K, Zilles K. 2008. Stereotaxic  
623 probabilistic maps of the magnocellular cell groups in human basal forebrain.  
624 *Neuroimage* 42(3):1127-41.

625

626